Mechanism of Homogeneous Iridium-Catalyzed Alkylation of Amines with Alcohols from a DFT Study

David Balcells,[†] Ainara Nova,[‡] Eric Clot,[†] Dinakar Gnanamgari,[§] Robert H. Crabtree,[§] and Odile Eisenstein*,[†]

Institut Charles Gerhardt, CNRS, UM2, cc 1501, Université Montpellier 2, 34095 Montpellier, France, Departament de Química, Universitat Autònoma de Barcelona, 08193 Bellatera, Spain, and Department of Chemistry, Yale University, New Haven, Connecticut 06520

Received February 14, 2008

The reaction mechanism for the Ir-catalyzed alkylation of primary amines with primary alcohols has been studied by DFT calculations. The three-step reaction pathway consists of Ir-catalyzed alcohol dehydrogenation to aldehyde, amine-aldehyde condensation to imine, and then Ir-catalyzed imine hydrogenation to amine. The presence of two essentially mirror-image reactions (dehydrogenation of the alcohol and hydrogenation of the imine) makes the reaction intrinsically challenging. The reaction is however shown to favor the product-forming direction because the dehydrogenation of an alcohol via β-H elimination has a lower barrier than the dehydrogenation of an amine. The prediction that amine dissociation is rate determining is consistent with the faster rate experimentally found here for the weakly basic amine $TsNH_2$. The ancillary carbonate ligand on Ir is shown to be involved in the hydrogen transfer. The two hydrogen atoms eliminated from the alcohol and added to the imine are transferred as H^- and H^+, the hydride going to and from the metal and the proton to and from the carbonate base.

Introduction

Alkylation of amines, a fundamental transformation in organic chemistry, is of particular interest for the pharmaceutical industry since hundreds of drugs contain alkylamino functions.[1] The traditional synthetic routes[2] via substitution with alkyl halides[3] or via reductive amination[4] are efficient but can involve mutagenic halides and the generation of much waste. Moreover, polyalkylation can lead to low selectivity.[5] Improved environmentally friendly methods are thus eagerly sought.[6] In response, metal-catalyzed alkylation of amines with alcohols (see Scheme 1) has been developed recently. Several advantages are apparent:

Scheme 1. Ir-Catalyzed N-Alkylation by Alcohols (top) and Its Proposed "Hydrogen-Borrowing" Mechanism (bottom)

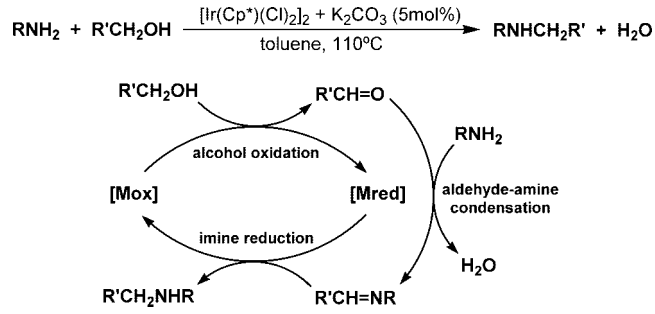

alcohols are readily available, monoalkylated products can be obtained with high selectivity, and the approach is much greener since fewer toxic reagents are needed and the only byproduct is water.

Several metal complexes have been developed for the catalytic alkylation of amines with alcohols,[7,8] one of the best known being $[Cp^*IrCl_2]_2$, as reported by Fujita et al.[9] (Scheme 1). Aryl and alkyl amines can be easily alkylated in good yields with several primary alcohols, typically using potassium carbon-

* Corresponding author. E-mail: odile.eisenstein@univ-montp2.fr.
[†] Université Montpellier 2.
[‡] Universitat Autònoma de Barcelona.
[§] Yale University.

(1) *Amines: Synthesis, Properties, and Application*; Lawrence, S. A., Ed.; Cambridge University Press: Cambridge, 2004.
(2) Salvatore, R. N.; Yoon, C. H.; Jung, K. W. *Tetrahedron* **2001**, *57*, 7785–7811.
(3) (a) Hartwig, J. F. *Synlett* **2006**, 1283–1294. (b) Buchwald, S. L.; Mauger, C.; Mignani, G.; Scholz, U. *Adv. Synth. Catal.* **2006**, *348*, 23–39. (c) Navarro, O.; Marion, N.; Mei, J.; Nolan, S. P. *Chem.−Eur. J.* **2006**, *12*, 5142–5148. (d) Ramiandrasoa, F.; Milat, M.-L.; Kunesch, G.; Chuilon, S. *Tetrahedron Lett.* **1989**, *30*, 1365–1368. (e) Li, X.; Mintz, E. A.; Bu, X. R.; Zehnder, O.; Bosshard, C.; Gunter, P. *Tetrahedron* **2000**, *56*, 5785–5791. (f) Wolfe, J. P.; Buchwald, S. L. *J. Am. Chem. Soc.* **1997**, *119*, 6054–6058.
(4) (a) Storer, R. I.; Carrera, D. E.; Ni, Y.; MacMillan, D. W. C. *J. Am. Chem. Soc.* **2006**, *128*, 84–86. (b) Abdel-Magid, A. F.; Carson, K. G.; Harris, B. D.; Maryanoff, C. A.; Shah, R. D. *J. Org. Chem.* **1996**, *61*, 3849–3862. (c) Tararov, V. I.; Börner, A. *Synlett* **2005**, 203–211. (d) Pelter, R.; Rosser, T.; Mills, N. *J. Chem. Soc., Perkin Trans. 1* **1984**, 717–720. (e) Pechulis, A. D.; Bellevue, F. H., III; Cioffi, C. L; Trapp, S. G.; Fojtik, J. P.; McKitty, A. A.; Kinney, W. A.; Frye, L. L. *J. Org. Chem.* **1995**, *60*, 5121–5126. (f) Vogel, S.; Stembera, K.; Hennig, L.; Findeisen, M.; Giesa, S.; Welzel, P.; Tillier, C.; Bonhomme, C.; Lampilas, M. *Tetrahedron* **2001**, *57*, 4147–4160. (g) Mizuta, T.; Sakaguchi, S.; Ishii, Y. *J. Org. Chem.* **2005**, *70*, 2195–2199.
(5) (a) Mitsunobu, O. *Comprehensive Organic Synthesis*; Trost, B. M., Fleming, I., Eds.; Pergamon: Oxford, 1991; Vol. 6, p 65. (b) Salvatore, R. N.; Nagle, A. S.; Jung, K. W. *J. Org. Chem.* **2002**, *67*, 674–683.
(6) Constable, D. J. C.; Dunn, P. J.; Hayler, J. D.; Humphrey, G. R.; Leazer, J. L.; Linderman, R. J.; Lorenz, K.; Manley, J.; Pearlman, B. A.; Wells, A.; Zaks, A.; Zhang, T. Y. *Green Chem.* **2007**, *9*, 411–420.
(7) (a) Roundhill, D. M. *Chem. Rev.* **1992**, *92*, 1–27. (b) Hamid, M. H. S. A.; Slatford, P. A.; Williams, J. M. J. *Adv. Synth. Catal.* **2007**, *349*, 1555–1575.
(8) (a) Grigg, R.; Mitchell, T. R. B.; Sutthivaiyakit, S.; Tongpenyai, N. *J. Chem. Soc. Chem. Commun.* **1981**, 611–612. (b) Watanabe, Y.; Tsuji, Y.; Ohsugi, Y. *Tetrahedron Lett.* **1981**, *22*, 2667–2670.
(9) (a) Fujita, K.; Li, Z.; Ozeki, N.; Yamaguchi, R. *Tetrahedron Lett.* **2003**, *44*, 2687–2690. (b) Fujita, K.; Yamamoto, K.; Yamaguchi, R. *Org. Lett.* **2002**, *4*, 2691–2694. (c) Fujita, K.; Fujii, T.; Yamaguchi, R. *Org. Lett.* **2004**, *6*, 3525–3528. (d) Yamaguchi, R.; Kawagoe, S.; Asai, C.; Fujita, K. *Org. Lett.* **2008**, *10*, 181–184. (e) Fujita, K.; Yamaguchi, R. *Synlett* **2005**, 560–571.

10.1021/om800134d CCC: $40.75
Publication on Web 05/08/2008

ate as mild base, to give the monoalkylated secondary amine products with very high selectivity, although relatively high temperatures (e.g., 110 °C) are required. Other iridium,[10] rhodium,[10c] and platinum[11] catalysts are also known. Heterogenous catalysts are also used to perform this transformation, but much higher pressures and temperatures are required.[12,13] Milder conditions are possible with certain Ru complexes:[10c,14] for example, Beller and co-workers have reported several $Ru_3(CO)_{12}$−phosphine combinations[14a] and Williams and coworkers have reported several [Ru(*p*-cymene)Cl_2]−phosphine and −diphosphine combinations,[14c] also with carbonates as base. Milstein has reported a different Ru catalyst that converts an alcohol and an amine to an amide and H_2, presumably going by a related reaction mechanism.[15]

The "hydrogen-borrowing" mechanism[7b,16] is generally accepted for hydrogen-transfer reactions.[17] This mechanism, previously postulated for the Cp*$IrCl_2$-catalyzed N-alkylation by alcohols (see Scheme 1), involves three sequential steps: (1) oxidation of the alcohol to aldehyde (eq 1; only primary alcohols are employed), (2) condensation of the aldehyde with the amine cosubstrate generating an imine (eq 2), and (3) reduction of the imine to the final amine product (eq 3).

$$RCH_2OH \rightarrow RCH{=}O + 2[H] \quad (1)$$

$$RCH{=}O + R'NH_2 \rightarrow RCH{=}NR' + H_2O \quad (2)$$

$$RCH{=}NR' + 2[H] \rightarrow RCH_2NHR' \quad (3)$$

Reactions 1 and 3 are the key steps of the mechanism that require the participation of the iridium catalyst. Because K_2CO_3 is a preferred base in the system,[9] we postulate Cp*$Ir(CO_3)$ as the catalyst (see Scheme 2). This complex contains a carbonate anion as a chelating bidentate ligand in place of Cl.

We find a viable pathway involving the mechanism represented in Scheme 2. We show that Cp*$Ir(CO_3)$ catalyzes the oxidation of the alcohol (eq 1) and the reduction of the imine (eq 3). Alcohol oxidation requires proton transfer to the carbonate ligand and hydride transfer to the metal by β-H elimination to give the aldehyde. After imine formation (eq 2), hydride transfer from the metal and proton transfer from bicarbonate gives the amine product. Amine dissociation to regenerate the catalyst is hard and, as the rate-determining step, accounts for the high temperatures needed to achieve acceptable rates.[9]

Scheme 2. "Hydrogen-Borrowing" Mechanism Postulated for the Carbonate Catalyst

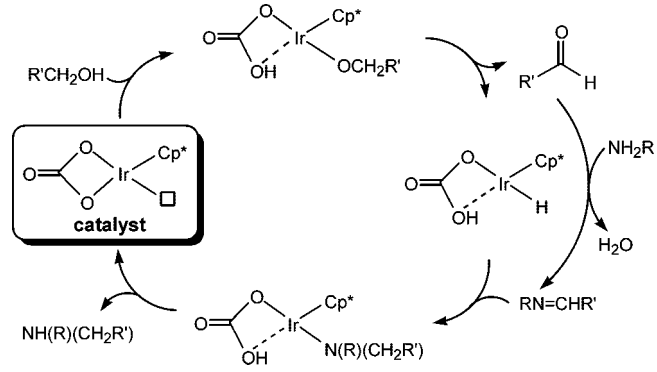

Computational Details

DFT calculations were carried out using the hybrid B3PW91 functional.[18] The basis set was the ECP-adapted SDDALL[19] with a set of polarization functions for Ir[20] and Cl[21] and the all-electron 6-31G(d,p)[22] for N, O, C, and H. Geometry optimizations were carried out without any geometrical constraints. The analytical calculation of frequencies was performed in order to classify each stationary point as minimum (reagents, catalysts, and intermediates) or transition state. Each transition state was relaxed toward reactant and product using the vibrational data to confirm its nature. The zero-point, thermal, and entropy corrections were evaluated to compute enthalpies and Gibbs free energies. The effect of the toluene solvent, which is weakly coordinating and of low polarity ($\epsilon = 2.379$), was evaluated using the continuum CPCM model.[23] All these energies are given in the Supporting Information. It was verified that the gas-phase potential energy profiles are similar to both the CPCM(toluene) and free energy profiles. All energies given in the text are thus the potential energies in the gas phase. The electronic structure of selected stationary points was analyzed through natural bond orbital (NBO) analysis, in which natural localized molecular orbitals (NLMO) were computed. All calculations were carried out with the Gaussian03 package.[25]

Results and Discussion

Reaction Modeling. The reaction of Scheme 1 involves four different components: the alcohol and amine reactants, K_2CO_3 as base, and the iridium catalyst. In the calculations, the

(10) (a) Cami-Kobeci, G.; Williams, J. M. J. *Chem. Commun.* **2004**, 1072–1073. (b) Cami-Kobeci, G.; Slatford, P. A.; Whittlesey, M. K.; Williams, J. M. J. *Bioorg. Med. Chem. Lett.* **2005**, *15*, 535–537. (c) Tanaka, N.; Hatanaka, M.; Watanabe, Y. *Chem. Lett.* **1992**, 575–578.

(11) Tsuji, Y.; Takeuchi, R.; Ogawa, H.; Watanabe, Y. *Chem. Lett.* **1986**, 293–294.

(12) (a) Botta, N.; de Angelis, D.; Nicoletti, R. *Synthesis* **1977**, 722–723. (b) Rice, R. G.; Kohn, E. J. *J. Am. Chem. Soc.* **1955**, *77*, 4052–4054. (c) Winans, C. F.; Atkins, H. *J. Am. Chem. Soc.* **1932**, *54*, 306–312.

(13) (a) Vultier, R. E.; Baiker, A.; Wokaun, A. *Appl. Catal.* **1987**, *30*, 167–176. (b) Baiker, A.; Kijenski, J. *Catal. Rev. Sci. Eng.* **1985**, *27*, 653–697. (c) Baiker, A.; Richarz, W. *Tetrahedron Lett.* **1977**, *18*, 1937–1938.

(14) (a) Tillack, A.; Hollmann, D.; Michalik, D.; Beller, M. *Tetrahedron Lett.* **2006**, *47*, 8881–8885. (b) Hollmann, D.; Tillack, A.; Michalik, D.; Jackstell, R.; Beller, M. *Chem. Asian J.* **2007**, *2*, 403–410. (c) Hamid, M. H. S. A.; Williams, J. M. J. *Chem. Commun.* **2007**, 725–727. (d) Naskar, S.; Bhattacharjee, M. *Tetrahedron Lett.* **2007**, *48*, 3367–3370.

(15) Gunanathan, C.; Ben-David, Y.; Milstein, D. *Science* **2007**, *317*, 790–792.

(16) (a) Clapham, S. E.; Hadzovic, A.; Morris, R. H. *Coord. Chem. Rev.* **2004**, *248*, 2201–2237. (b) Samec, J. S. M.; Bäckvall, J.-E. E.; Andersson, P. G.; Brandt, P. *Chem. Soc. Rev.* **2006**, *35*, 237–248.

(17) (a) Gladiali, S.; Alberico, E. *Chem. Soc. Rev.* **2006**, *35*, 226–236. (b) Noyori, R.; Hashiguchi, S. *Acc. Chem. Res.* **1997**, *30*, 97–102. (c) Zassinovich, G.; Mestroni, G.; Gladiali, S. *Chem. Rev.* **1992**, *92*, 1051–1069. (d) Brieger, G.; Nestrick, T. J. *Chem. Rev.* **1974**, *74*, 567–580. (e) *Hydrogen-Transfer Reactions*; Hynes, J. T., Klinman, J. P., Limbach, H.-H., Schowen, R. L., Eds.; Wiley-VCH: Weinheim, 2006.

(18) (a) Becke, A. D. *J. Chem. Phys.* **1993**, *98*, 5648–5662. (b) Perdew, J. P.; Wang, Y. *Phys. Rev. B* **1992**, *45*, 13244–13249.

(19) (a) Andrae, D.; Haüssermann, U.; Dolg, M.; Stoll, H.; Preuss, H. *Theor. Chim. Acta* **1990**, *77*, 123–141. (b) Bergner, A.; Dolg, M.; Küchle, W.; Stoll, H.; Preuss, H. *Mol. Phys.* **1993**, *80*, 1431–1441.

(20) Ehlers, A. W.; Böhme, M.; Dapprich, S.; Gobbi, A.; Höllwarth, A.; Jonas, V.; Köhler, K. F.; Stegmann, R.; Veldkamp, A.; Frenking, G. *Chem. Phys. Lett.* **1993**, *208*, 111–114.

(21) Höllwarth, A.; Böhme, H.; Dapprich, S.; Ehlers, A. W.; Gobbi, A.; Jonas, V.; Köhler, K. F.; Stegmann, R.; Veldkamp, A.; Frenking, G. *Chem. Phys. Lett.* **1993**, *203*, 237–240.

(22) Hariharan, P. C.; Pople, J. A. *Theor. Chim. Acta* **1973**, *28*, 213–222.

(23) (a) Barone, V.; Cossi, M. *J. Phys. Chem. A* **1998**, *102*, 1995–2001. (b) Tomasi, J.; Mennucci, B.; Cammi, R. *Chem. Rev.* **2005**, *105*, 2999–3094.

(24) Reed, A. E.; Curtiss, L. A.; Weinhold, F. *Chem. Rev.* **1988**, *88*, 899–926.

Scheme 3. Iridium Species Considered As Catalyst Models

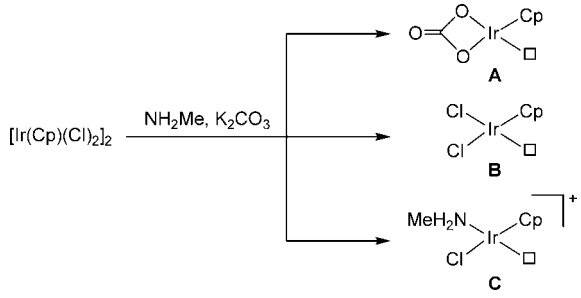

experimental C_5Me_5 ligand (Cp*) is modeled by C_5H_5 (Cp), while methanol and methylamine are used to model the reagents. Apart from $CpIr(CO_3)$ (**A**), we have explored the pathways for the neutral $CpIrCl_2$ monomer (**B**) and the cationic $CpIr(NH_2Me)(Cl)^+$ complex (**C**), which could also be present in the reaction media (see Scheme 3). Several general trends have emerged from exploring these limiting possibilities.

Carbonate-Assisted Alcohol Oxidation. Coordination of the alcohol to the κ^2-carbonate cyclopentadienyl complex **A** catalyst leads to the formation of the **A**−**IN1** intermediate (see Figure 1), in which the metal is bound to methanol with an Ir−O bond of 2.22 Å. This associative step is moderately exothermic by 8.0 kcal mol^{-1} and does not affect the chelating κ^2-character of the carbonate. Intermediate **A**−**IN1** is also stabilized by a H-bond involving the acidic hydrogen of the alcohol and one of the Ir-bound oxygens of carbonate. With its short OH···O distance of 1.93 Å, this intermediate is well prepared for proton transfer from the alcohol to the carbonate. At the transition state for the proton transfer, **A**−**TS1**, the proton is located between the alcohol and carbonate oxygens (d(MeO···H) = 1.31 Å and d(OC(O)O···H) = 1.14 Å), closer to the carbonate. This transition state connects to intermediate **A**−**IN2**, containing an alkoxy and a κ^1-bicarbonate ligand. Intermediate **A**−**IN2** is a 16*e* complex with a planar Ir center, as shown by the sum of 360° for the three bond angles at Ir. The proton transfer is exothermic by −2.1 kcal mol,$^{-1}$ allowing the coordinated carbonate to deprotonate the alcohol, a reaction that would not have been possible between the weakly basic free carbonate and the weakly acid free alcohol. The energy barrier is moderate, as is appropriate for proton transfer.

The transition state **A**−**TS3** for β-H elimination (C···H = 1.51 Å and Ir···H 1.65 Å) of the alkoxy bicarbonato intermediate **A**−**IN2** has been located at an energy of 7.5 kcal mol^{-1} above separated reactants. This transition state does not connect directly to **A**−**IN2** but to an isomer, **A**−**IN3**, in which the alkoxy group is agostic (C···H = 1.21 Å and Ir···H = 1.87 Å). The transition state **A**−**TS2** between the nonagostic alkoxy complex **A**−**IN2** and **A**−**IN3** has an energy only marginally

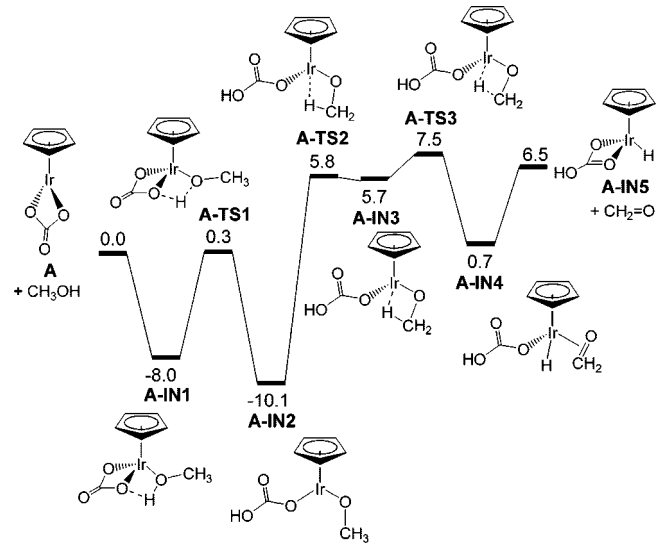

Figure 1. Alcohol Oxidation Pathway with Catalyst **A**.

higher than the agostic intermediate and has a similar geometry (C···H = 1.16 Å and Ir···H = 2.05 Å). Even though **A**−**IN3** is thus a transient rather than a fully fledged intermediate, it shows that the major component of the barrier for β-H elimination is the bending of the Ir−O−C(methyl) angle, yielding an agostic CH−Ir interaction.

The transition state **A**−**TS3** leads to a hydride formaldehyde complex, **A**−**IN4**, having a π-bonded H_2C=O (Ir···O = 2.09 Å and Ir···C = 2.14 Å). The release of H_2C=O from **A**−**IN4** requires only 5.8 kcal mol^{-1} because formaldehyde is a weak ligand and because of the chelation of the bicarbonate in **A**−**IN5**. The overall oxidation process (**A** + CH_3OH → **A**−**IN5** + CH_2=O) is endothermic by only 6.5 kcal mol^{-1}. The highest point along the reaction pathway corresponds to the β-H elimination transition state, **A**−**TS3** (7.5 kcal mol^{-1} above reactants), during which a C−H bond of the alkoxy ligand is activated. The β-H elimination is thus the rate-determining step in the alcohol oxidation.

These calculations show that complex **A** is able to promote the oxidation of methanol to formaldehyde through a low-energy pathway. In accord with these results, Fujita reported recently that a similar {Cp*Ir} complex catalyzes the oxidation of several alcohols.[26] Interestingly, the carbonate ligand is directly involved in the oxidation process, taking one of the hydrogens of the substrate as a proton. The active role of some ancilliary ligands in catalytic processes has been previously proposed for acetate[27] and carbonate[28] on the basis of theoretical and experimental studies. Similarly, concerted proton and hydride transfer has been proposed for the reduction of imines and carbonyl

(25) Frisch, M. J.; Trucks, G. W.; Schlegel, H. B.; Scuseria, G. E.; Robb, M. A.; Cheeseman, J. R.; Montgomery, Jr., J. A.; Vreven, T.; Kudin, K. N.; Burant, J. C.; Millam, J. M.; Iyengar, S. S.; Tomasi, J.; Barone, V.; Mennucci, B.; Cossi, M.; Scalmani, G.; Rega, N.; Petersson, G. A.; Nakatsuji, H.; Hada, M.; Ehara, M.; Toyota, K.; Fukuda, R.; Hasegawa, J.; Ishida, M.; Nakajima, T.; Honda, Y.; Kitao, O.; Nakai, H.; Klene, M.; Li, X.; Knox, J. E.; Hratchian, H. P.; Cross, J. B.; Bakken, V.; Adamo, C.; Jaramillo, J.; Gomperts, R.; Stratmann, R. E.; Yazyev, O.; Austin, A. J.; Cammi, R.; Pomelli, C.; Ochterski, J.; Ayala, P. Y.; Morokuma, K.; Voth, G. A.; Salvador, P.; Dannenberg, J. J.; Zakrzewski, V. G.; Dapprich, S.; Daniels, A. D.; Strain, M. C.; Farkas, O.; Malick, D. K.; Rabuck, A. D.; Raghavachari, K.; Foresman, J. B.; Ortiz, J. V.; Cui, Q.; Baboul, A. G.; Clifford, S.; Cioslowski, J.; Stefanov, B. B.; Liu, G.; Liashenko, A.; Piskorz, P.; Komaromi, I.; Martin, R. L.; Fox, D. J.; Keith, T.; Al-Laham, M. A.; Peng, C. Y.; Nanayakkara, A.; Challacombe, M.; Gill, P. M. W.; Johnson, B. G.; Chen, W.; Wong, M. W.; Gonzalez, C.; Pople, J. A. *Gaussian 03*, (Revision D.01); Gaussian, Inc.: Wallingford, CT, 2004.

(26) Fujita, K.; Tanino, N.; Yamaguchi, R. *Org. Lett.* **2007**, *9*, 109–111.

(27) (a) Davies, D. L.; Donald, S. M. A.; Macgregor, S. A. *J. Am. Chem. Soc.* **2005**, *127*, 13754–13755. (b) Davies, D. L.; Donald, S. M. A.; Al-Duaij, O.; Macgregor, S. A.; Polleth, M. *J. Am. Chem. Soc.* **2006**, *128*, 4210–4211.

(28) (a) Garcia-Cuadrado, D.; Braga, A. A. C.; Maseras, F.; Echavarren, A. M. *J. Am. Chem. Soc.* **2006**, *128*, 1066–1067. (b) Garcia-Cuadrado, D.; de Mendoza, P.; Braga, A. A. C.; Maseras, F.; Echavarren, A. M. *J. Am. Chem. Soc.* **2007**, *129*, 6880–6866. (c) Ozdemir, I.; Demir, S.; Cetinkaya, B.; Gourlaouen, C.; Maseras, F.; Bruneau, C.; Dixneuf, P. H. *J. Am. Chem. Soc.* **2008**, *130*, 1156–1157.

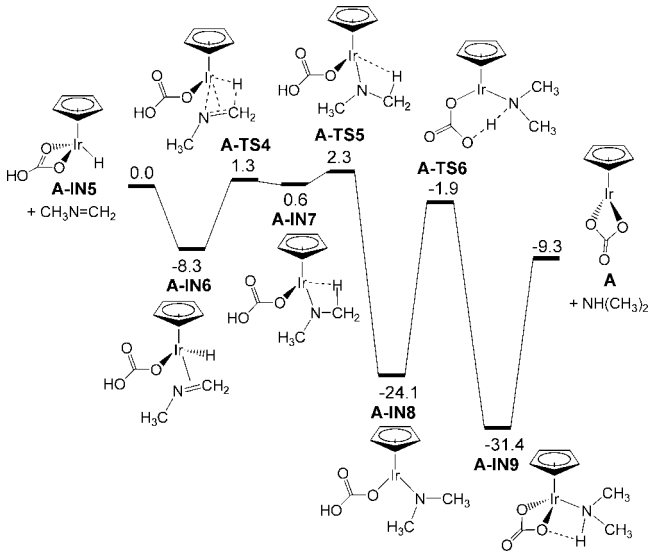

Figure 2. Imine reduction pathway with catalyst **A**.

compounds with the Shvo catalyst, involving the hydroxycyclopentadienyl ligand.[29,30]

Imine Formation. The product of the Ir-assisted alcohol oxidation, CH_2═O, reacts with the amine cosubstrate (NH_2Me), giving rise to water and CH_3N═CH_2 (see Scheme 2). We have not modeled this step because it is a standard organic condensation reaction. The only special feature here is that it occurs in refluxing toluene, not in the polar solvents that are usually required.[31] However, the presence of alcohol and amine in the medium may provide a sufficiently polar microenvironment or, alternatively, the reaction may be metal-catalyzed.

Carbonate-Assisted Imine Reduction. The imine reacts with the iridium hydride **A**−**IN5**, leading to the formation of complex **A**−**IN6**, in which the imine is bound to the metal[32] (Figure 2). In **A**−**IN6**, the imine is η^2-bonded and the carbonate is κ^1-bonded with Ir−O distances of 2.06 and 3.20 Å. The decoordination of one oxygen of the carbonate ligand is compensated by the imine coordination, as shown by the relative energies of **A**−**IN5** and free imine and **A**−**IN6**, 8.3 kcal mol^{-1} in favor of **A**−**IN6**.

The imine inserts into the Ir−H bond of **A**−**IN6**, yielding **A**−**IN8**, having an amido $N(CH_3)_2$ group. The amido complex is formed in a two-step process consisting of the formation of an agostic intermediate (**A**−**IN7** via **A**−**TS4**) followed by isomerization of the latter into a nonagostic complex **A**−**IN8** via **A**−**TS5**. This transformation, in which **A**−**IN7** is just a transient, has the two transition states, **A**−**TS4** and **A**−**TS5**, at 1.3 and 2.3 kcal mol^{-1} above reactants, respectively. Complex **A**−**IN7** is an unstable intermediate (0.6 kcal mol^{-1} above reactants) containing a C−H···Ir agostic interaction characterized by C−H and Ir−H bond distances of 1.23 and 1.80 Å, respectively. The nonagostic amido intermediate, **A**−**IN8**, is much more stable (24.1 kcal mol^{-1} below reactants) and has a short Ir−N bond of 1.91 Å (2.07 Å in **A**−**IN7**) and a planar Ir center, indicating formation of an Ir−N π-bond. The carbonate ligand remains coordinated in a κ^1-fashion throughout the insertion.

The κ^1-HCO_3 ligand protonates the NMe_2 group of **A**−**IN8** to give the amine product via the transition state **A**−**TS6**, at 1.9 kcal mol^{-1} below reactants, in which the proton lies midway between an O of the carbonate ligand and N (O···H 1.28 Å and N···H 1.19 Å). This proton transfer is moderately exothermic by 7.3 kcal mol.$^{-1}$ **A**−**TS6** leads to complex **A**−**IN9**, in which the coordinated product $NHMe_2$ (Ir−N 2.15 Å) is hydrogen bonded to a κ^2-carbonate (Ir−O 2.05 Å). Dissociation of the amine requires 22.1 kcal mol^{-1} and regenerates catalyst **A**. Overall, the imine reduction is exothermic by 9.3 kcal mol^{-1} and occurs with successive steps having accessible energy barriers.

Amine Coordination. The more basic amine reagent tends to outcompete the alcohol for binding to Ir: the dissociation energy of CH_3OH from CpIr(κ^2-CO_3)(CH_3OH), **A**−**IN1**, is 8.0 kcal mol^{-1} (Figure 1), while that of CH_3NH_2 from CpIr(κ^2-CO_3)(CH_3NH_2) is 23.4 kcal mol^{-1}. The amine therefore inhibits the reaction by disfavoring the coordination of the alcohol. The product of the reaction, $(CH_3)_2NH$, has almost the same Ir−N bond dissociation energy (22.1 kcal mol^{-1}; Figure 2) because it is more basic but also more bulky than CH_3NH_2. The amine also outcompetes the imine for coordination to **A**−**IN5**. The dissociation energy of the imine from **A**−**IN6** is 8.3 kcal mol^{-1} (Figure 2), whereas the dissociation of the amine from CpIrH(κ^1-HCO_3)(CH_3NH_2) costs 19.8 kcal mol.$^{-1}$ These results show that, apart from alcohol oxidation, the other step with a significant energy barrier is amine dissociation. As a result, high temperatures (110 °C) are required to achieve good rates. For a given amine there seems to be no remedy for this reagent inhibition of the reaction.

Moving to a less basic amine was therefore predicted to accelerate the reaction, and this proposal was successfully tested experimentally for the case of $TsNH_2$ (Ts = p-$CH_3C_6H_4SO_2$) versus the best studied case of $PhCH_2NH_2$. At short reaction times (see eq 4, R = $PhCH_2$ or Ts) that give 20% yield of the expected secondary amine from $PhCH_2NH_2$, we instead obtain a 53% yield of $PhCH_2NHTs$ from $TsNH_2$, implying a faster rate for this case. The latter version of the reaction is also significant in giving a protected primary amine rather than the secondary amines previously reported.

$$\underset{(1\ \text{mmol})}{PhCH_2OH} + \underset{(1\ \text{mmol})}{RNH_2} \xrightarrow[PhCH_3\ (0.5\ \text{mL, reflux, 2h})]{[Cp^*IrCl_2]_2\ (2.5\%),\ K_2CO_3\ (5\%)} PhCH_2NHR \qquad (4)$$

Symmetry of the Reaction Scheme. The reaction steps of eq 1 intrinsically mirror those of eq 3, so factors that favor one disfavor the other, complicating optimization of the whole scheme. The alcohol oxidation and imine reduction go via a β-H elimination from an alkoxy ligand and the insertion of the imine into the Ir−H bond. It is fortunate that the sequence of events is always slightly in favor of the formation of the products. For instance, the proton transfer is exothermic when the proton goes from the coordinated alcohol to the coordinated carbonate and from the bicarbonate to the amido group because of the order in Lewis basicity. Likewise the β-H elimination of the alkoxy group to form the aldehyde has a lower barrier (**A**−**IN2** → **A**−**TS2** $\Delta E^{\ddagger}$ = 15.9 kcal mol^{-1}) than the β-H transfer from the amido to the imine (**A**−**IN8** → **A**−**TS5** $\Delta E^{\ddagger}$ = 26.4 kcal mol^{-1}). Indeed, N-alkylation by amines requires

(29) (a) Shvo, Y.; Czarkie, D.; Rahamim, Y.; Chodosh, D. F. *J. Am. Chem. Soc.* **1986**, *108*, 7400–7402. (b) Casey, C. P.; Singer, S. W.; Powell, D. R.; Hayashi, R. K.; Kavana, M. *J. Am. Chem. Soc.* **2001**, *123*, 1090–1100.

(30) (a) Privalov, T.; Samec, J. S. M.; Bäckvall, J.-E. *Organometallics* **2007**, *26*, 2840–2848. (b) Comas-Vives, A.; Ujaque, G.; Lledos, A. *Organometallics* **2007**, *26*, 4135–4144.

(31) Hall, N. E.; Smith, B. J. *J. Phys. Chem. A* **1998**, *102*, 4930–4938.

(32) Samec, J. S. M.; Éll, A. H.; Åberg, J. B.; Privalov, T.; Eriksson, L.; Bäckvall, J.-E. *J. Am. Chem. Soc.* **2006**, *128*, 14293–14305.

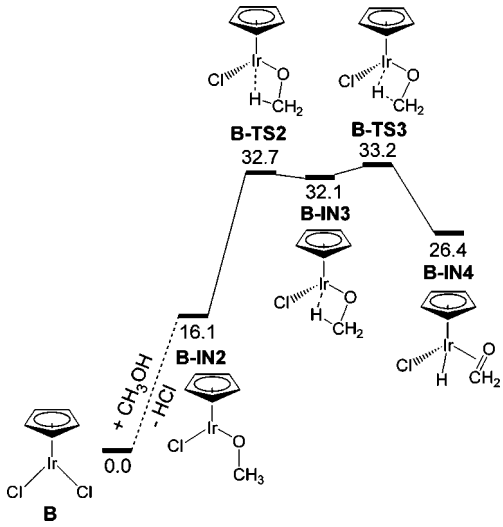

Figure 3. Energy profile for β-H elimination with complex **B**.

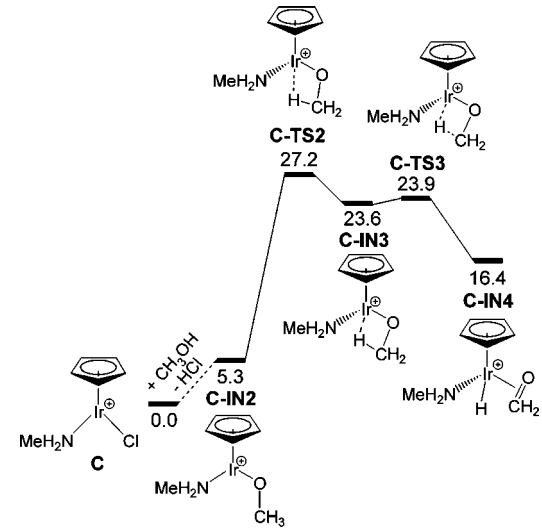

Figure 4. Energy profile for β-H elimination with complex **C**.

higher temperatures.[33] All these factors favor oxidation of the alcohol over that of the amine and reduction of the imine over that of the aldehyde.

This calculated trend in relative ease of oxidation of alcohols and amine is supported by a study by Casey et al. of reduction of carbonyl and imine by the hydroxycyclopentadienyl ruthenium hydride: reduction of imine is considerably faster than that of carbonyl.[29b] In this case the reduction occurs via concerted proton and hydride transfer, similar to that described here, the difference being the nature of the ligand involved in the proton transfer. As a consequence, even if amine is the most coordinating ligand, the alcohol is easier to oxidize than the amine and, by producing the aldehyde, promotes the forward reaction. In addition, the reaction proceeds to the final secondary amine because the imine is easier to reduce than the aldehyde.

Other Possible Active Forms of the Catalyst. The alkylation of NH_2Me by methanol was also explored with complexes **B** and **C** as catalysts (Scheme 3), focusing on the β-H elimination step. In the case of complex **B**, the formation of **B**−**IN2**, through an intermolecular proton transfer from coordinated methanol to Cl to liberate HCl (Figure 3 and eq 5), was not studied in detail.

$$\mathbf{B} + CH_3OH \rightarrow \mathbf{B}-\mathbf{IN2} + HCl \qquad (5)$$

The formation of **B**−**IN2** is endothermic by 16.1 kcal mol^{-1}, reflecting the weakly acidic character of methanol and the low basicity of chloride. The oxidation of the OMe ligand in **B**−**IN2** into O=CH_2 is a two-step process analogous to that found for catalyst **A**, requiring an energy barrier from **B**−**IN2** to **B**−**TS3** of 17.1 kcal mol^{-1}. The high-energy of **B**−**TS3** relative to the starting reagent (33.2 kcal mol^{-1}) and the high endothermicity of the transformation from **B** and CH_3OH to **B**−**IN4** (26.4 kcal mol^{-1}) show that the reaction with complex **B** is less favored than with complex **A**.

The same set of calculations was carried out using cationic complex **C** (Figure 4). The reaction starts with the protonation of the Cl ligand of **C** by CH_3OH according to eq 6 and the formation of the alkoxy complex **C**−**IN2**.

$$\mathbf{C} + CH_3OH \rightarrow \mathbf{C}-\mathbf{IN2} + HCl \qquad (6)$$

This initial step is moderately endothermic by 5.3 kcal mol^{-1}. From **C**−**IN2**, the β-H elimination occurs via the two step-reaction previously described, the only difference being that the highest transition state corresponds to the formation of the agostic methoxy group. The energy barrier of 21.9 kcal mol^{-1} relative to **C**−**IN2** (27.2 kcal mol^{-1} relative to **C** and CH_3OH) shows that the β-H elimination remains a step with a high energy barrier. The aldehyde complex **C**−**IN4** is 16.4 kcal mol^{-1} above reactants.

The oxidation of the alcohol is thus significantly preferred for the carbonate ligand (catalyst **A**). This is the only case where the formation of the alkoxy complex is favored relative to reactants. The β-H elimination has the lowest energy barrier also with the carbonate, and finally the endothermicity of the formation of the aldehyde complex relative to separated reagent is the smallest.

***β*-H Elimination from Ir−OMe and Ir−NMe_2.** A general point emerges from this study: β-H elimination from Ir−OMe and from Ir−NMe_2 in a 16*e* d^6 complex or intermediate is increasingly harder from alkoxy to amido ligand. A study by Macgregor and Vadivelu has addressed a closely related point.[34] The d^8 square-planar $IrX(CO)(PPh_3)_2$ undergoes β-H elimination at 0 °C for X = octyl, but only above 95 °C for X = OEt.[35] The DFT calculations by Macgregor and Vadivelu have shown that this is due to the presence of a π-interaction between Ir and the alkoxy group in the three-coordinate complex formed from loss of a phosphine ligand. This interaction deactivates the alkoxy complex toward β-H elimination. The absence of this stabilization in the alkyl complex is the reason for its higher reactivity. It has also been shown that $Cp^*Ru(PR_3)X$ (X = π-donor) has a mirror-symmetry structure with Ru, P, X, and the Cp* centroid coplanar because of the presence of a π-bond between Ru and X.[36] In addition, an MO analysis showed how the presence of a π-acceptor ligand leads to a pyramidal structure for $CpMn(CO)_2$.[37] A similar interpretation applies in the d^6 Ir complexes. In our case (Figure 1), this π-donation is favorable in the 16*e* precursor complex **A**−**IN2**, where an empty metal orbital is available, but cannot occur in the 18*e* intermediate

(33) Hollmann, D.; Bähn, S.; Tillack, A.; Beller, M. *Angew. Chem., Int. Ed.* **2007**, *46*, 8291–8294.

(34) Macgregor, S. A.; Vadivelu, P. *Organometallics* **2007**, *26*, 3651–3659.

(35) (a) Schwartz, J.; Cannon, J. B. *J. Am. Chem. Soc.* **1974**, *96*, 2276–2278. (b) Zhao, J.; Hesslink, H.; Hartwig, J. F. *J. Am. Chem. Soc.* **2001**, *123*, 7220–7227.

(36) Johnson, T. J.; Folting, K.; Streib, W. E.; Martin, J. D.; Huffman, J. C.; Jackson, S. A.; Eisenstein, O.; Caulton, K. G. *Inorg. Chem.* **1995**, *34*, 488–499.

(37) Hofmann, P. *Angew. Chem., Int. Ed. Engl.* **1977**, *16*, 536–537.

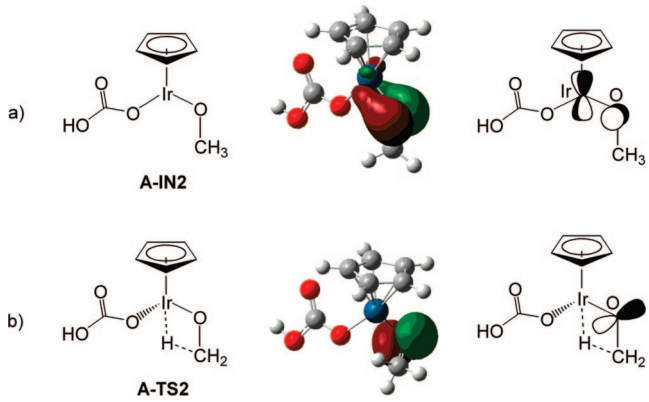

Figure 5. Graphical representation of the NLMO oxygen lone pair in **A−IN2** (a) and **A−TS2** (b) from an NBO analysis.

Table 1. NBO Analysis of the π-Donation of the X Lone Pair (X = O, N) to Iridium for the Intermediates and Transition States Associated with the β-H Elimination Step and Energy Barriers in kcal mol^{-1} for this Step[a]

	reactant		transition state		
reaction pathway	χ^{Ir}	χ^{x}	χ^{Ir}	χ^{x}	energy barrier
A−IN2 → A−TS2	7.4%	85.8%	0.9%	95.4%	15.9
A−IN5 → A−TS8	32.9%	64.2%	1.4%	94.4%	26.4
B−IN2 → B−TS2	8.0%	86.0%	0.9%	95.5%	16.6
C−IN2 → C−TS2	8.6%	84.4%	1.3%	94.6%	21.9

[a] χ^{Ir} and χ^{X} represent the contributions of the metal and X in the NLMO describing the X lone pair.

agostic complex **A−IN3** because the empty metal orbital is involved in the agostic interaction and where $d_\pi-p_\pi$ interactions are only 4*e* destabilizing. Therefore, the formation of the 18*e* complex in which the Ir−O π-bond is lost is the main cause for the high energy barrier of the β-H elimination step, as shown by the fact that the transition states for this step (**A−TS3**) and the agostic complex (**A−IN3**) have the same energy (15.9 and 15.8 kcal mol^{-1}, respectively).

This change in the Ir−O interaction from **A−IN2** to **A−TS2** is supported by the significant lengthening of the Ir−O bond (1.92 Å in **A−IN2** and 2.00 Å in **A−TS2**). It is also confirmed by an NBO analysis. In **A−IN2**, the six metal electrons are located in d_{xy}, $d_{x^2-y^2}$, and d_{z^2} (where the *z* axis lies on the Ir−Cp centroid vector and the O atoms lie in the *yz* plane). In addition to the Ir−O σ-bond, the Ir−methoxy bond includes a π-delocalization of the O lone pair into the Ir d_{xz} orbital, as illustrated by the NLMO lone pair shown in Figure 5. The formation of the agostic complex at **A−TS2** is associated with bending of the Ir−O−C angle to 90° and pyramidalization at Ir (Ir is no longer in the plane defined by the cyclopentadienyl centroid and the two coordinated oxygen atoms). Consequently, the empty metal orbital no longer overlaps with the oxygen lone pair, preventing the establishment of an Ir−O π-bond. This point is clearly reflected by the contributions of iridium (χ^{Ir}) and oxygen (χ^{O}) to the NLMO representing the lone pair: χ^{Ir} decreases from 7.4% to 0.9% along the **A−IN2 → A−TS2** pathway, whereas χ^{O} increases from 85.8% to 95.4% (see Table 1).

For clarity, we discuss the β-H elimination of the amido ligand in the same direction as for the alkoxide case even though the reverse reaction occurs (the amido complex **A−IN8** is formed during the reaction by reduction of the imine complex **A−IN6**). The β-H elimination from **A-IN8** via **A-TS5** has an energy barrier of 26.4 kcal mol^{-1}, clearly higher than for the methoxy ligand (**A−IN2 → A−TS2**, $\Delta E^{\ddagger} = 15.9$ kcal mol^{-1}). Indeed amido complexes rarely undergo β-H elimination or become agostic.[38] Because the N lone pair is at higher energy than that of the oxygen, the Ir−N π-bond is stronger and all effects found in the case of Ir−OCH_3 are stronger for the amido ligand (Table 1). In fact, the NBO procedure did find a Ir−N π-bond in **A−IN8**.

The same analysis applies to the **B** and **C** forms of the catalyst. Only the β-H elimination from the alkoxy group was examined (**IN2** to **TS2**). The ancillary ligand tunes the Ir−O π-bond. If the ancillary ligand is itself a π-donor, it competes with the alkoxy group, the Ir−O π-bond in **IN2** is weaker, and the energy barrier for β-H elimination is lower. The chloride (**B**) and the bicarbonate (**A**), having similar π-donating ability, have similar energy barriers. In contrast, if the ancillary ligand has no π-donor effect and in addition the complex is positively charged, as is the case for **C**, the Ir−O π-bond in **IN2** is stronger and the barrier for β-H elimination higher. The direct relation between the magnitude of the loss of the π-bond from the unsaturated intermediate **IN2** to **TS2** as evaluated by NBO analysis and the energy barrier for β-H elimination is shown by the values in Table 1.

Conclusion

The reaction pathway for the Ir-catalyzed N-alkylation of amines by alcohols has computed reaction barriers consistent with the experimental requirement for elevated temperatures. The reaction is composed of three multistep reactions: (1) Ir-catalyzed oxidation of the alcohol, (2) nucleophilic addition of the amine to the aldehyde, and (3) Ir-catalyzed reduction of the imine to the final secondary amine. During these steps, coordination of the alcohol and the imine to the metal center is required. However the amines present as reactant and as product are both better Lewis bases than either the alcohol or the imine. Thus amine dissociation from the metal, required to regenerate the catalyst, is hard, and this step may account for the high temperature required. This result led to a successful experimental test with the weakly basic amine $TsNH_2$, which reacts at a faster rate, consistent with easier $TsNH_2$ dissociation.

The reaction consists of two transfomations that are mirror-images of each other: the same catalyst has to dehydrogenate the alcohol and hydrogenate the imine. Improving one of the reactions is expected to be deleterious for the other, and therefore improving the overall process may be challenging. The presence of a carbonate as ancillary ligand has been found to lower the energy barrier of many steps. It participates in the dehydrogenation of the alcohol by hosting the proton while the hydride coordinates to the metal. It has the reverse effect of proton reservoir for the reduction of the imine. The presence of such a ligand has already been found to be important for alcohol dehydrogenation. Carbonate can easily go from κ^2 to κ^1 as a function of the metal coordination. Proton transfer to and from the ligand to be oxidized or reduced has been the object of considerable attention, but this aspect cannot be properly treated by computations due to the impossibility of representing all equilibria between the different bases present. We merely show here how carbonate can play this role.

The dehydrogenation of an alcohol via proton transfer and β-H elimination has been shown to have a lower barrier than that for an amine. This is related to the weaker Ir−O π-bond in the alkoxy intermediate relative to the Ir−N π-bond in an amido intermediate. This contributes to the production of the required aldehyde by selective oxidation of the alcohol rather than the

(38) Hartwig, J. F. *Acc. Chem. Res.* **1998**, *31*, 852–860.

amine. In contrast, the imine formed from the condensation of the aldehyde and the amine is more easily hydrogenated to the secondary amine than is an aldehyde. These preferences contribute to favoring the forward direction of the overall process.

Experimental Section

General Comments. All the operations were carried out under a nitrogen atmosphere using standard Schlenk techniques. Toluene was distilled from sodium-benzophenone. All starting materials and reagents were obtained from commercial sources and used as received unless otherwise noted. All glassware was dried overnight prior to use. ^{1}H, ^{13}C, and ^{31}P NMR spectra were obtained using a Bruker spectrometer operating at 400 or 500 MHz. $[Cp^*IrCl_2]_2$ was prepared according to the method of Heinekey.[39]

Procedure. An oven-dried flask under an atmosphere of nitrogen was charged with $[Cp^*IrCl_2]_2$ (0.025 mmol), 1,3,5-trimethoxy benzene as internal standard, and K_2CO_3 (0.050 mmol) in toluene (0.5 mL). The amine (1.00 mmol) and the alcohol (1.00 mmol) were then added, and the mixture was refluxed for 2 h and then extracted with CH_2Cl_2 (1.00 mL). The extract was filtered through Celite, evaporated to dryness, and redissolved in CD_2Cl_2 (0.30 mL). The products were then analyzed by NMR spectroscopy by comparison with authentic materials. The conversion is based on a comparison with the internal standard.

Acknowledgment. We all thank Sanofi-Aventis, for funding and for suggesting the problem. Additional support came from the CNRS and the Ministère de l'Enseignement Supérieur et de la Recherche (D.B., A.N., E.C., and O.E.) and the U.S. DOE (R.H.C. and D.G.). D.B. also thanks Sanofi-Aventis for a postdoctoral position, and A.N. also thanks the Spanish MEC for financing her stay in Montpellier.

Supporting Information Available: Cartesian coordinates of all optimized geometries reported in the text, together with their potential, CPCM(toluene), and Gibbs free energies.

OM800134D

(39) Ball, R. G.; Graham, W. A. G.; Heinekey, D. M.; Hoyano, J. K.; McMaster, A. D.; Mattson, B. M.; Michel, S. T. *Inorg. Chem.* **1990**, *29*, 2023–2025.